Solid State Ionics 230 (2013) 48–51

Contents lists available at SciVerse ScienceDirect

Solid State Ionics

journal homepage: www.elsevier.com/locate/ssi

Ionic conductivity and phase stability of spark plasma sintered scandia and ceria-stabilized zirconia

R.L. Grosso [a], M. Bertolete [b], I.F. Machado [b], R. Muccillo [a], E.N.S. Muccillo [a,*]

[a] Energy and Nuclear Research Institute, S. Paulo, 05508-000, SP, Brazil
[b] Polytechnique School, University of S. Paulo, S. Paulo, 05508-010, SP, Brazil

ARTICLE INFO

Article history:
Received 30 April 2012
Received in revised form 10 July 2012
Accepted 2 August 2012
Available online 7 September 2012

Keywords:
Zirconia
Spark plasma sintering
Crystalline structure
Microstructure
Impedance spectroscopy

ABSTRACT

In this work the effect of sintering on the ionic conductivity of scandia and ceria-stabilized zirconia, ScCeSZ, is investigated. Commercial ScCeSZ with specific surface area of 11.5 $m^2.g^{-1}$ was used as received. Consolidation of the solid electrolyte was accomplished by spark plasma sintering in the 1273–1473 K range for 1 and 5 min. The relative sintered density for spark plasma sintered samples was higher than 95% for temperatures of 1373 K and higher. Raman spectroscopy analysis revealed that all samples exhibit both cubic and tetragonal structures. The ionic conductivity was systematically evaluated by impedance spectroscopy and the main difference in the blocking of O^{2-} ions at the grain boundary of several samples is related to the average grain size. In the high-temperature range, a decrease in the ionic conductivity with increasing dwell temperature and time is attributed to the increase of the fraction of tetragonal phase.

1. Introduction

Stabilized zirconias are well-known solid electrolytes with several applications in electrochemical devices such as solid oxide fuel cells and solid oxide electrolyzers. Scandia-stabilized zirconia is reported to exhibit the highest ionic conductivity in zirconia-based solid electrolytes [1] and therefore is a candidate material for application in solid oxide fuel cells operating at intermediate temperatures (~870–1070 K). The crystal structure of this system is complex [2–4] and several attempts have been done to stabilize the cubic phase at room temperature. Recently, addition of minor amounts of Al_2O_3, TiO_2, Bi_2O_3 and CeO_2 was investigated for this purpose [5–8].

Addition of ceria to scandia-stabilized zirconia reduces its electrical conductivity, although it remains higher than that of yttria-stabilized zirconia in the intermediate temperature range [9]. Moreover, the additive is found to improve the phase stability of the system [10].

The sintering of this solid electrolyte is usually carried out at high temperatures (above 1670 K) to obtain suitable densification for the proposed application. Few reports concerning the use of spark plasma sintering to scandia-stabilized zirconia may be found elsewhere [11–13]. The main results were related to the stabilization of the cubic structure at room temperature and the suppression of grain growth in the sintered materials [11,12]. The decrease of the electrical conductivity in the high temperature region and the simultaneous increase of that parameter at low temperatures have also been reported [11,13].

To the best of our knowledge no reports on the use of this consolidation technique may be found for ternary systems. In this work, the effect of spark plasma sintering on the electrical conductivity and phase stability of scandia and ceria-stabilized zirconia is investigated. The main purpose of this work is to obtain dense and fine-grained ceramics with suitable electrical conductivity.

2. Experimental

Zirconia containing 10 mol% scandia and 1 mol% ceria (ScCeSZ-TS, Fuel Cell Materials), with 11.5 $m^2.g^{-1}$ of specific surface area, was used as received. Consolidation of the pellets was accomplished by spark plasma sintering (SPS 1050, Sumitomo Coal Mining Co., Japan). In a typical processing cycle, ScCeSZ powder was loaded into a graphite die lined with graphite sheets. The die containing powder was heated with the simultaneous application of pressure up to the desired temperature (1273, 1373 and 1473 K) by a pre-set program. The maximum applied pressure was 65 MPa, which was released after the dwell time (1 or 5 min). Heating and cooling rates in SPS consolidations were 100 and 300 $K.min^{-1}$, respectively.

The sintered density was determined by the immersion method. Structural characterization of sintered pellets was carried out by X-ray diffraction (Bruker-AXS, D8 Advance) in the 20–80° 2θ range with CuK_α radiation, and by Raman spectroscopy (Renishaw, InVia Raman Microscope) coupled to a Leica optical microscope, with an excitation radiation of 633 nm from a He–Ne laser. Microstructural observations were performed in a field emission scanning electron microscope, FE-SEM (Jeol, JSM 6701F). The mean grain size, *G*, was estimated by the intercept method [14]. The ionic conductivity was

* Corresponding author at: Instituto de Pesquisas Energéticas e Nucleares-IPEN, PO Box 11049, S. Paulo, SP, 05422-970, Brazil. Tel.: +55 11 31339203; fax: +55 11 31339276.
E-mail address: enavarro@usp.br (E.N.S. Muccillo).

0167-2738/$ – see front matter © 2012 Elsevier B.V. All rights reserved.
http://dx.doi.org/10.1016/j.ssi.2012.08.006

Table 1
Values of sintered density (ρ_H) and mean grain size (G) of samples consolidated by SPS at several dwell temperatures and times.

Dwell temperature (K)	Dwell time (min)	ρ_H (%)	G (μm)
1273	5	74.3 ± 0.2[a]	~0.1[b]
1373	5	95.7 ± 0.1	0.31 ± 0.03
1473	1	96.5 ± 0.1	0.36 ± 0.04
1473	5	97.1 ± 0.1	0.42 ± 0.05

[a] Relative geometric density.
[b] Estimated from the fractured surface.

determined by impedance spectroscopy measurements using a low-frequency impedance analyzer (4192A Hewlett Packard) in the 5 Hz to 13 MHz frequency range. Silver and platinum pastes were used as electrode materials in the low- (573–723 K) and high-temperature (723–1073 K) measurements, respectively.

3. Results and discussion

Table 1 shows the relative sintered density values of ScCeSZ samples consolidated at different dwell temperatures and times. A huge increase of approximately 20% occurred in the sintered density between 1273 and 1373 K, and beyond that the increase in density is comparatively small. Moreover, the increase in the dwell time from 1 to 5 min at 1473 K did not offer any substantial advantage concerning the densification of ScCeSZ.

Fig. 1 shows FE-SEM micrographs of SPS samples. In the case of the sample sintered at 1273 K only the fractured surface could be observed (Fig. 1a). In this sample, the porosity is randomly distributed and the estimated mean grain size is about 0.1 μm. The polished and thermally etched surface of the samples sintered at higher temperatures exhibits similar features, namely low porosity and homogeneous distribution of grain sizes. The grains are of polygonal shape and no exaggerated grain growth is observed. Fig. 1b shows, as an example, the micrograph of the sample consolidated at 1473 K for 5 min. Increase in both dwell temperature and time resulted in increase of the mean grain size (Table 1).

X-ray diffraction patterns of ScCeSZ samples are shown in Fig. 2a. These profiles seem to be characteristics of the cubic phase of stabilized-zirconia (JCPDS 89-5483). In the low-angle region of the main diffraction peak a slight broadening may be observed. To clarify about the origin of this effect, about 50 μm of the sample surface was removed by grinding and X-ray diffraction patterns were again recorded. No differences were observed between the X-ray diffraction patterns measured before and after grinding. The samples were, then, analyzed by Raman spectroscopy, a technique that allows for a better identification of the structural phases in zirconia matrices. Fig. 2b shows Raman spectra of the ScCeSZ samples. The Raman spectrum of cubic zirconia displays a single band at ~620 cm^{-1} [8]. As can be seen, an additional band at ~480 cm^{-1} reveals the presence of the tetragonal phase in these samples [3]. The Raman band marked with (*) is a further evidence of the phase composition. This band at approximately 700 cm^{-1} was detected in scandia-stabilized zirconia with tetragonal symmetry, and was attributed to some type of disorder due to formation of the solid solution and consequent generation of oxygen vacancies [3].

Fig. 3 shows impedance spectroscopy diagrams of ScCeSZ sintered samples at 650 K (low-temperature region). These diagrams were normalized for sample dimensions, and the numbers over experimental points refer to the logarithm of the frequency (Hz). In this temperature range the grain and the grain boundary contributions

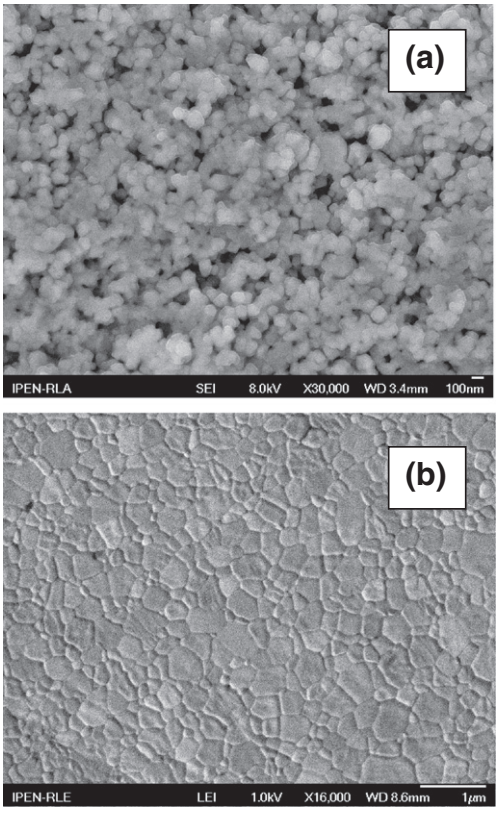

Fig. 1. FE-SEM micrographs of ScCeSZ samples consolidated by SPS: a) fractured surface of the sample sintered at 1273 K/5 min; b) polished and etched surface of the sample sintered at 1473 K/5 min.

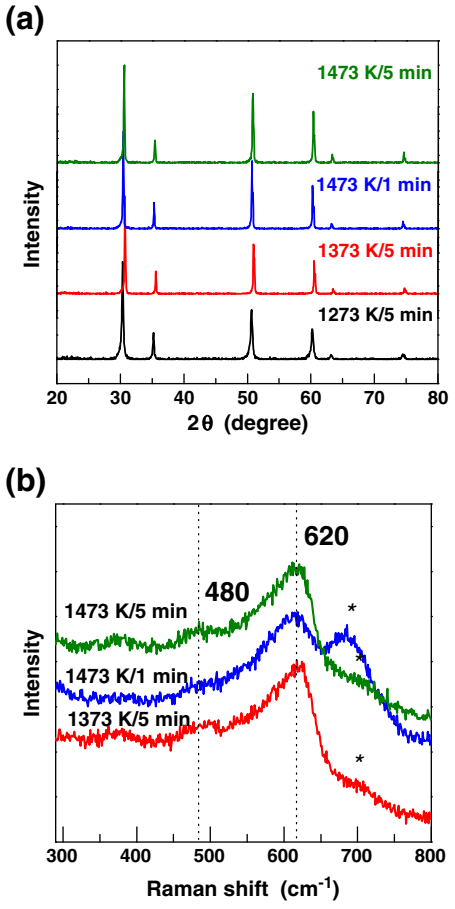

Fig. 2. (a) X-ray diffraction patterns and (b) Raman spectra of ScCeSZ samples.

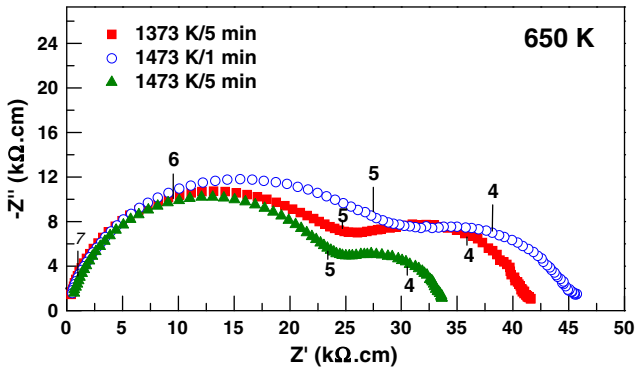

Fig. 3. Impedance spectroscopy diagrams of ScCeSZ samples at 650 K. Numbers over experimental points are the logarithm of the frequency.

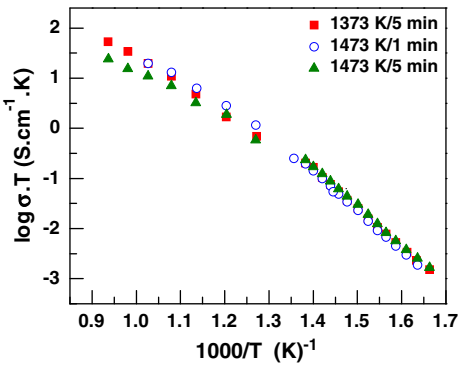

Fig. 5. Arrhenius plots of the overall electrical conductivity of ScCeSZ samples.

to the overall electrolyte conductivity were deconvoluted. The main difference in the samples sintered at the same temperature and different dwell times is related to the grain boundary blocking effect. Increasing the sintering time resulted in decreasing the blocking effect. The same phenomenon is observed with increasing dwell temperature.

The Arrhenius plots of the grain conductivity are shown in Fig. 4a. As expected, the grain (or intragranular) conductivity remains unchanged independent on dwell temperature and time. Apparent activation energy values obtained by fitting resulted in 1.55 ± 0.04 eV, in general agreement with previous works [8,9]. In order to evaluate the effect of grain size on the blocking effect at grain boundaries, correction of the corresponding electrical conductivity for the grain boundary surface according to [15] was carried out and the results are shown in Fig. 4b. The Arrhenius plots of the consolidated samples show a similar behavior and small differences between them may be ascribed to uncertainties in the measured dimensions and slightly differing contents of the tetragonal phase. It may be concluded then that the grain boundary surface accounts for the blocking effect at the grain boundaries in ScCeSZ sintered by the SPS process.

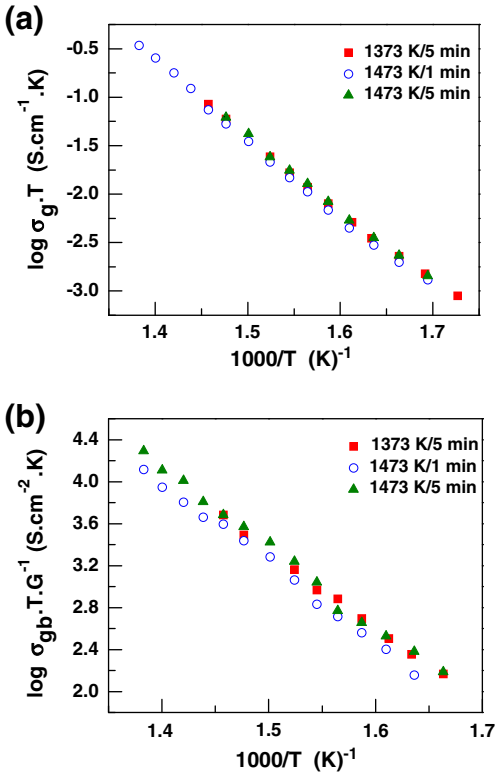

Fig. 4. Arrhenius plots of the electrical conductivity of (a) grains and (b) normalized grain boundaries. *G* stands for the mean grain size.

Fig. 5 shows the Arrhenius plots of the overall (grain and grain boundary) conductivity of ScCeSZ samples in the whole temperature range of measurements. For this experiment, platinum was used as electrode material. The overall electrical conductivity of the samples is quite similar at low temperatures (up to ~723 K). In the high temperature range (~723–1073 K) the sample sintered at 1473 K for 5 min exhibits a small decrease in the electrical conductivity. This effect may be explained as a consequence of formation of the tetragonal phase, as detected by Raman spectroscopy. Reduction of Ce^{4+} to Ce^{3+} that might have occurred during SPS experiments due to the reduced atmosphere inside the pressure chamber may account for this effect. Increasing the temperature and time in SPS experiments should increase the fraction of tetragonal phase. The CeO_2 additive employed to stabilize the cubic phase at room temperature, in this case, could no longer be effective to fully stabilize the solid electrolyte. Apparent activation energy values of the overall electrolyte conductivity in the high temperature region are 1.15 ± 0.05 (1373 K/5 min and 1473 K/1 min) and 0.84 ± 0.04 eV (1473 K/5 min). This latter value is similar to that obtained for zirconia–12 mol% scandia [8].

4. Conclusions

High density and submicron zirconia–scandia–ceria specimens have been obtained by spark plasma sintering at temperatures higher than 1270 K. The tetragonal phase that has been detected by Raman spectroscopy might be responsible for the decrease in the overall electric conductivity. An explanation of the cubic-to-tetragonal phase transition is set forth based on Ce^{4+}–Ce^{3+} conversion in the graphite die during the spark plasma sintering process.

Acknowledgments

The authors acknowledge FAPESP, CNEN and CNPq for financial supports, the Laboratory of Molecular Spectroscopy of the University of S. Paulo, for Raman measurements, and the Laboratory of Electron Microscopy of IPEN for SEM observations. One of the authors (R. L. G.) acknowledges CAPES for the scholarship.

References

[1] T.H. Etsel, S.N. Flengas, Chem. Rev. 70 (1970) 339.
[2] M. Yashima, M. Kakihana, M. Yoshimura, Solid State Ionics 86–88 (1996) 1131.
[3] H. Fujimori, M. Yashima, M. Yoshimura, J. Am. Ceram. Soc. 81 (1998) 2885.
[4] K. Du, C. Kim, A.H. Heuer, J. Am. Ceram. Soc. 91 (2008) 1626.
[5] C. Haering, A. Roosen, H. Schichl, M. Schnöller, Solid State Ionics 176 (2005) 261.
[6] J. Kondoh, Y. Tomii, K. Kawachi, J. Am. Ceram. Soc. 86 (2003) 2093.
[7] Y. Arachi, T. Asai, O. Yamamoto, Y. Takeda, N. Imanishi, K. Kawate, C. Tamakoshi, J. Electrochem. Soc. 148 (2001) A520.
[8] F. Tietz, W. Fischer, Th. Hauber, G. Mariotto, Solid State Ionics 100 (1997) 289.

[9] Z. Wang, M. Cheng, Z. Bi, Y. Dong, H. Zhang, J. Zhang, Z. Feng, C. Li, Mater. Lett. 59 (2005) 2579.
[10] D.S. Lee, W.S. Kim, S.H. Choi, J. Kim, H.-W. Lee, J.-H. Lee, Solid State Ionics 176 (2005) 33.
[11] M. Okamoto, Y. Akimune, K. Furuya, M. Hatano, M. Yamanaka, M. Uchiyama, Solid State Ionics 176 (2005) 675.
[12] K. Biswas, Ceram. Int. 35 (2009) 2047.
[13] T. Shimonosono, H. Kimura, Y. Sakka, J. Ceram. Soc. Jpn. 118 (2010) 1038.
[14] M.I. Mendelson, J. Am. Ceram. Soc. 52 (1969) 443.
[15] M. Miyayama, H. Inoue, H. Yanagida, J. Am. Ceram. Soc. 66 (1983) C164.